



저작자표시-비영리-동일조건변경허락 2.0 대한민국

이용자는 아래의 조건을 따르는 경우에 한하여 자유롭게

- 이 저작물을 복제, 배포, 전송, 전시, 공연 및 방송할 수 있습니다.
- 이차적 저작물을 작성할 수 있습니다.

다음과 같은 조건을 따라야 합니다:



저작자표시. 귀하는 원저작자를 표시하여야 합니다.



비영리. 귀하는 이 저작물을 영리 목적으로 이용할 수 없습니다.



동일조건변경허락. 귀하가 이 저작물을 개작, 변형 또는 가공했을 경우에는, 이 저작물과 동일한 이용허락조건하에서만 배포할 수 있습니다.

- 귀하는, 이 저작물의 재이용이나 배포의 경우, 이 저작물에 적용된 이용허락조건을 명확하게 나타내어야 합니다.
- 저작권자로부터 별도의 허가를 받으면 이러한 조건들은 적용되지 않습니다.

저작권법에 따른 이용자의 권리는 위의 내용에 의하여 영향을 받지 않습니다.

이것은 [이용허락규약\(Legal Code\)](#)을 이해하기 쉽게 요약한 것입니다.

[Disclaimer](#)

공학석사 학위논문

Solution-Grown Homojunction Oxide Thin-Film Transistors of Superior Electrical Performance

우수한 전기특성을 지닌 용액공정 기반의
호모정션 트랜지스터

2019 년 8 월

서울대학교 대학원

융합과학부 나노융합전공

이 준 희

Solution-Grown Homojunction Oxide Thin-Film Transistors of Superior Electrical Performance

지도 교수 김 연 상

이 논문을 공학석사 학위논문으로 제출함
2019 년 8 월

서울대학교 대학원
융합과학부 나노융합전공
이 준 희

이준희의 공학석사 학위논문을 인준함
2019 년 6 월

위 원 장 _____ 박 원 철 _____ (인)

부위원장 _____ 김 연 상 _____ (인)

위 원 _____ 송 윤 규 _____ (인)

Abstract

Solution-Grown Homojunction Oxide Thin-Film Transistors of Superior Electrical Performance

Junhee Lee

Program in Nano Science and Technology

The Graduate School

Seoul National University

Growing attention has been granted to solution-grown metal oxide thin film transistors of low temperature annealing, since they can be applied in the emerging sector of large-scale and flexible electronics. Recently, the expanded uses of solution-processed devices face limitations relating to their inferior carrier transportation and unsuitable operating characteristics. I overcome these hindrances through a renovated structure called “homojunction” consisting of a channel layer and a channel-electron modulation layer. Not only do I accomplish solution-grown oxide thin-film transistors with markedly higher mobility values than other reported solution-grown transistors, but I also demonstrate a turn-on voltage of the homojunction oxide

transistors can be effectively controlled through modifying each layer. Furthermore, outstanding achievements associated with reliability, stability and uniformity are verified. These outcomes are ascribed to the remarkable phenomena of solution-grown thin films. Our findings highlight the indium oxide thin films of high quality can be yielded through solution process at low annealing temperature, and thus solution-grown indium oxide transistors hold great promise for widespread industrial applications.

Keyword : Homojunction, Oxide Thin-Film Transistor, Solution Process, High Field-Effect Mobility, Turn-on Voltage

Student Number : 2017-26594

Table of Contents

Abstract	1
Table of Contents.....	3
List of Figures	5
Chapter 1. Introduction.....	7
1.1 Study Background of Metal Oxide	7
1.2 Purpose of Homojunction Transistor.....	9
Chapter 2. Experimental Section.....	10
2.1 Precursor Solution Synthesis and Deposition Tech- niques	10
2.2 Transistor Fabrication and Characterization.....	11
2.3 Material Characterization Techniques	12
Chapter 3. Results and Discussion	13
3.1 Structure of Homojunction Oxide TFTs.....	13
3.2 Phenomenal Facts of Homojunction.....	15
3.2.1 Superior Electrical Characteristics of Solution- Grown Homojunction Oxide TFTs.....	15
3.2.2 Tendencies for Electrical Performance of Homo- junction Oxide TFTs	17
3.2.3 Admirable other device traits: Stability and Uniformity	20

3.3 Origin of the Outstanding Results	22
3.3.1 Investigation in Phase of Thin Films by XRD ...	22
3.3.2 Analysis of Homojunction through HR-TEM ...	24
3.3.3 Inquiry about Single Oxide Thin Film Layer via AFM and XPS.....	26
3.3.4 Examination of Density by using XRR.....	32
3.4 Influences on Solution-Grown Oxide Thin Films ...	34
3.4.1 Single-Layered Oxide Thin Film	34
3.4.2 Homojunction Oxide Thin Film.....	36
3.5 Application: NMOS Inverter	38
Chapter 4. Conclusion.....	40
Reference	42
초록(국문)	46

List of Figures

Figure 1. Schematic structure of homojunction oxide TFTs.

Figure 2. (A) Transfer curve of single-layered and homojunction oxide TFTs (B) Comparison of an average field-effect mobility from various solution-grown oxide TFTs.

Figure 3. The inclination of homojunction oxide TFTs for (A) μ_{FE} and (B) V_{on} depending on diverse conditions of channel layers.

Figure 4. The tendency of homojunction oxide TFTs toward (A) μ_{FE} and (B) V_{on} according to the modification of a CEML.

Figure 5. Reliability and uniformity of homojunction TFTs. (A) Electrical characteristics of homojunction lasting more than 50 days. (B) Histogram plot of μ_{FE} by 25 transistors of homojunction with In_2O_3 (0.1 M) / In_2O_3 (0.1 M).

Figure 6. XRD characteristics of In_2O_3 films annealed at 250°C and 200°C.

Figure 7. HR-TEM cross-section images of Si/SiO₂/ In_2O_3 (0.1 M) / In_2O_3 (0.1 M) homojunction oxide TFT.

Figure 8. Height profile of various single-layered oxide thin films. (A) 0.05 M, (B) 0.1 M, (C) 0.15 M, (D) 0.2 M, (E) 0.25 M single-layered In_2O_3 thin films. (F) Height distributions derived from the AFM data.

Figure 9. Surface topography of In_2O_3 thin films. (A) 0.05 M, (B) 0.1 M, (C) 0.15 M, (D) 0.2 M, (E) 0.25 M single-layered In_2O_3 thin films. (F) RMS distributions extracted from the AFM images.

Figure 10. Elemental depth profile of the thick single-layered In_2O_3 thin film (~15 nm) stack on the Si/ SiO₂ substrate.

Figure 11. Formation process of solution-grown oxide thin

films. (A) Schematic diagram from as-deposited to fully developed oxide films. XPS analysis of (B) surface and (C) bulk binding energy of 15 nm single-layered In_2O_3 thin films.

Figure 12. Density profile of single-layered In_2O_3 thin films depending on molar concentration of precursors.

Figure 13 The influences of a surface charge effect and defects on single-layered oxide TFTs. Schematic images and electrical hysteresis of (A) High quality single films under 11 nm, (B) Low quality single films above 11 nm.

Figure 14. The impacts of defects and a surface charge effect on homojunction oxide TFTs. Schematic diagrams and electrical hysteresis of (A) homojunction TFTs with amorphous CEML ($\text{a-In}_2\text{O}_3$), and of (B) homojunction TFTs with crystalline CEML ($\text{C-In}_2\text{O}_3$).

Figure 15. (A) Schematic architecture and (B) Voltage transfer characteristics of a solution-processed NMOS inverter consisting of two homojunction oxide TFTs.

.

Chapter 1. Introduction

1.1. Study Background of Metal Oxide

Oxide Semiconductors (OSs) have regarded cutting-edge materials for next-generation electronics, including transparent smart windows, mobile displays, solar cells and transparent metal oxide diodes, due to their high optical transparency, high carrier mobility, tunable energy bandgap and deposition process versatility.¹⁻⁷ Nowadays OSs were produced in vacuum process such as radio frequency (RF) sputtering, pulsed laser deposition (PLD), atomic layer deposition (ALD) in spite of various methods to deposit OSs. One of the main reasons for exploiting such system was that vacuum deposition process forms high-quality thin films of dense and low defects, causing outstanding electrical performances and sustaining their characteristics.^{8,9} However, the vacuum systems were inevitably expensive because of the equipment which makes and maintains a high degree vacuum state, indicating the necessity of employing cheap and simplicity growth process.^{5,10,11}

Simple process and low cost in producing OS films were one of merits of using solution process, not utilizing vacuum equipment and a complicated process such as photolithography. Especially, low temperature solution deposition processes have obtained huge attentions because they were considered to be appropriate for a continuous, large-scale next-generation industry such as roll-to-roll process.^{10,12-14} Although low temperature solution deposition method has various advantages, the solution processes have not been industrialized on the ground that OSs from the solution process exhibit poor electrical performances compared to vacuum-

processed ones. Since precursors consisting of various components were used for solution methods, a huge amount of impurities regarded as defects in electronic state was an unavoidable consequence, causing the inferior electrical performance.^{5,15} To enhance electrical characteristics of low temperature solution-grown thin films, many studies have been performed with a focus on eliminating impurities without increasing annealing temperature.

It has been demonstrated that solution-processed oxide films of few impurities can be produced through various approaches such as ultraviolet (UV) annealing, developing precursors and combustion methods.¹⁵⁻¹⁸ Although they successfully fabricate oxide thin films of few defects, solution-processed oxide thin films still display inferior electrical performance as compared to vacuum-deposited oxide ones. The main reason seems that a small amount of orbital overlap came from both voids and porous structures.^{15,19} To overcome such hindrances, recent studies have introduced diverse techniques, including high pressure annealing, doping of foreign atoms and structure with two different materials, can help to reach the level of electrical characteristics of vacuum-processed devices.¹⁹⁻²⁴

Specifically, solution-processed oxide films with double layer hold great promise as an alternative of state-of-the-art vacuum-processed oxide ones since double-stacked oxide films have achieved high electrical properties.²²⁻²⁴ Although this method helps to achieve notable improvement of electrical characteristics, the researches on the double-stacked structure are still in initial stage. Because little has been found in terms of roles of layers and their impacts on electrical performance. Therefore, this indicates the necessity of additional studies on double-stacked oxide thin films.

1.2. Purpose of Homojunction Transistor

Herein, I propose a novel structure called “Homojunction” , solution coating with different film quality of material, not only to obtain superior electrical performances comparable to state-of-the-art devices but to sustain their characteristics. By controlling a film quality of channel and channel-electron modulation layer (CEML) and consequently manipulating electrical characteristics, I argue that films from a solution process can be formed with a different quality depending on their level of as-deposited thickness. Finding the optimized quality of films, I can achieve the highest field effect mobility or near 0 V V_{on} . Moreover, the homojunction can be produced at low temperature annealing (250°C), and its electrical performances can be maintained more than 50 days. I have utilized thin-film transistor (TFT), well known demonstration procedure, in a method to prove electrical characteristics. This study claims that oxide films from solution process have a potential of being applied for advanced transistor channel.

Chapter 2. Experimental Section

2.1. Precursor Solution Synthesis and Deposition Techniques

Indium nitrate hydrate $[\text{In}(\text{NO}_3)_3 \cdot \text{H}_2\text{O}]$ (99.999%, Sigma-Aldrich) were dissolved in deionized (DI) water to form In_2O_3 precursor solutions (0.05 M, 0.1 M, 0.15 M, 0.2 M, 0.25 M) and after that, the precursors were stirred at 500 rpm for 3 days. To fabricate oxide thin films, I used the spin coating where its parameters were 5000 rpm for 30 s at a humidity under $\sim 10\%$. The humidity means the relative humidity at 25°C . A 0.22 mm syringe filter PTFE (DISMIC 13HP020AN, Advantec, Japan) were utilized to filter In_2O_3 precursor. As-deposited amorphous (polycrystalline) films were soft-baked at 200 (250) $^\circ\text{C}$ for 1 min, and then subjected into tube furnace to anneal for 8 (4) hours at 200 (250) $^\circ\text{C}$. All chemicals were used as received.

2.2. Transistor Fabrication and Characterization

Homojunction oxide TFTs were developed in bottom-gate, top-contact structure on highly B-doped Si wafers with a thickness of 200 nm thermally developed layer of SiO₂ as a role of the gate electrode and the gate dielectric, respectively. The wafers were rinsed by subsequent ultrasonication in detergent for 15 min, DI water cleansing for 1 hours, ultrasonication in acetone, and isopropanol for 15 min each, followed by ultraviolet/ozone treatment for 20 min. Deposition procedure of the In₂O₃ layers was performed using the methods in Section 2.1. Agilent 4155B semiconductor parameter analyser estimated the output and transfer electrical characteristics of homojunction oxide TFT under dark condition. The field-effect mobility (μ_{FE}) of homojunction TFTs was calculated by the linear formula.

2.3. Material characterization techniques

The thickness and roughness of In_2O_3 thin films were measured using AFM (XE100, PSIA). I used XRR (SmartLab, Rigaku Co.) to obtain the density of In_2O_3 thin films with Cu-K α radiation ($\lambda = 1.54$ Å) at 45 kV and 200 mA. GlobalFit program was utilized to obtain XRR fitting data. To check the phase of materials, XRD (D8 Advance, Bruker Co.) was implemented with Cu-K α radiation ($\lambda = 1.54$ Å) at 40 kV and 150 mA (6 kW) and grazing-incidence mode. The XPS spectra were acquired in a AXIS Supra (Kratos, U.K.) system equipped with a monochromic AlK α x-ray source. Depth profile analysis was carried out by mild, destructive in situ sputter etching using Ar $^+$ beam of 5kV to achieve the required depth resolution. The specimens for HR-TEM observation were prepared by ion beam processing techniques through Quanta 3D FEG. A platinum plated layer with thickness of 15 nm was deposited via sputter before TEM specimen preparation to cause its surface more conductive. The HR-TEM images were all acquired by JEM-2100F field emission electron microscope from JEOL Ltd.

Chapter 3. Results and Discussion

3.1. Structure of Homojunction oxide TFTs

As shown in Figure 1, a homojunction oxide TFT is a bottom-gate and top-contact transistor with a solution-grown $\text{In}_2\text{O}_3/\text{In}_2\text{O}_3$ where each layer is called as a CEML and a channel layer, respectively. I utilized a highly boron-doped silicon wafer as a gate electrode and a substrate. A silicon dioxide (SiO_2) of 200 nm thickness was thermally oxidized on the wafer as a role of gate dielectric. The homojunction layers of solution-grown $\text{In}_2\text{O}_3/\text{In}_2\text{O}_3$ were fabricated on the SiO_2 layer via subsequent spin-coated depositions of In_2O_3 precursors under 5 percent humidity. The solution-grown In_2O_3 films consisting of the homojunction oxide TFTs are constructed by using different molar concentration In_2O_3 precursors. Thicknesses of the films are dependent on the different precursors and material phase of thin films are altered through adjustment of annealing temperature. For source and drain electrodes, the channel width and length of thermally evaporated aluminum are 300 μm and 300 μm , respectively.

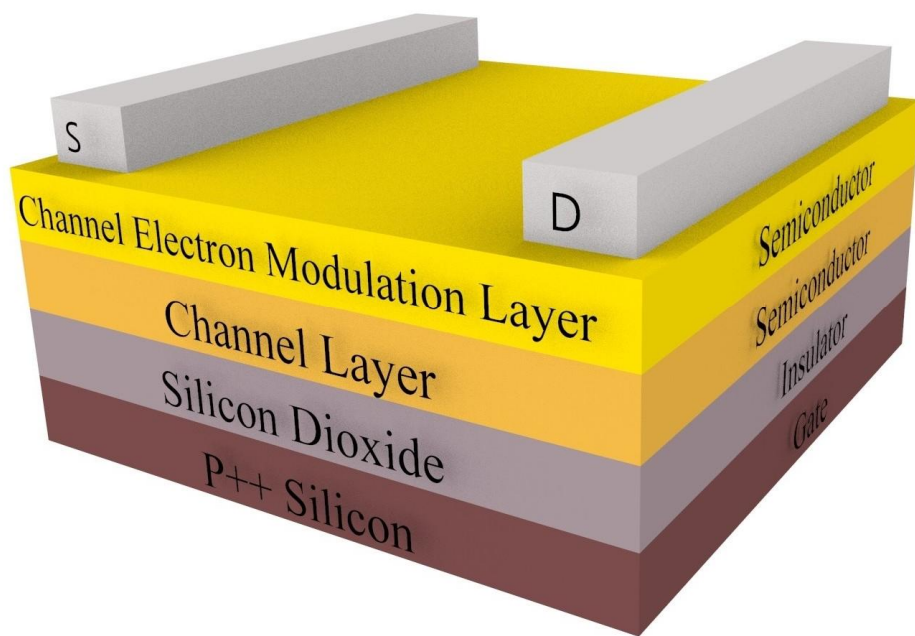


Figure 1. Schematic structure of Homojunction oxide TFTs.

3.2. Phenomenal Facts of Homojunction

3.2.1 Superior Electrical Characteristics of Solution-Grown Homojunction Oxide TFTs

One of the outstanding outcomes of the homojunction structure is that the solution-grown homojunction oxide TFTs can control its V_{on} , while keeping their high μ_{FE} , through modulating a CEML and a channel layer. I successfully make the homojunction oxide TFTs having significantly larger currents without large variation of V_{on} by optimizing process conditions of each layer, most likely because of the improved electron mobility, than solution-grown amorphous and polycrystalline single-layered In_2O_3 oxide TFTs (Figure 2A). Analyzing transfer characteristics of single-layered In_2O_3 and the homojunction oxide TFTs shows that μ_{FE} of the In_2O_3/In_2O_3 homojunction oxide TFTs is nearly $50 \text{ cm}^2/V \cdot s$, and that of the amorphous (polycrystalline) single-layered In_2O_3 TFTs is 2.7 (8.3) $\text{cm}^2/V \cdot s$. All single-layered metal oxide and the homojunction oxide TFTs represent a conventional n-channel behavior with on/off ratios of 10^6 . Amorphous and polycrystalline single-layered In_2O_3 TFTs hold their own electrical characteristics according to the molar concentration of precursors, which is similar results proven by previous work.²⁵ Examination of electrical performance in Figure 2A reveals that μ_{FE} of the In_2O_3/In_2O_3 homojunction oxide TFTs outperform that of other reported oxide TFTs (Figure 2B).²²⁻²⁴ The μ_{FE} of the solution-grown homojunction oxide TFTs shows approximately 6 times higher than polycrystalline single-layered In_2O_3 TFTs and 1.5 times higher than the cutting-edge, high performing solution-grown heterojunction oxide TFTs.²⁴

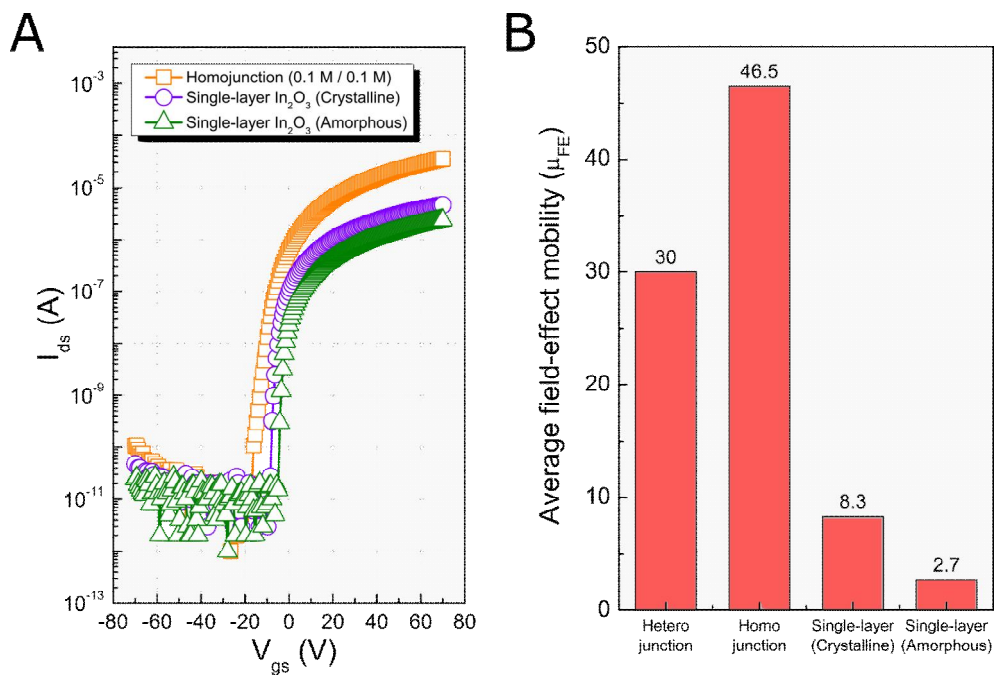


Figure 2. (A) Transfer curve of single-layered and homojunction oxide TFTs (B) Comparison of an average field-effect mobility from various solution-grown oxide TFTs.

3.2.2 Tendencies for Electrical Performance of Homojunction Oxide TFTs

The trends for electrical performance of the solution-grown homojunction oxide TFTs with various conditions are displayed from Figure 3 to Figure 4. Interestingly, the homojunction architectures, where channel layers are changed with 0.05 M, 0.1 M, 0.15 M, 0.2 M, 0.25 M when the condition of CEML is 0.1 M, represent unusual events in the area of μ_{FE} (Figure 3A). Analogous μ_{FE} should have been obtained when the identical material is operated for the channel since free electrons accumulated near the semiconductor/dielectric interface dominated the mobility.^{26,27} However, the thicker a film was, the poorer its electrical characteristics were attained because of the variance in film quality, which I will explain later. Another types of homojunction oxide TFTs, where channel layer was fixed in In_2O_3 using 0.1 M and CEMLs were varied with 0.05 M, 0.1 M, 0.15 M, 0.2 M and 0.25 M, showed different inclinations that μ_{FE} was maintained regardless of CEML conditions (Figure 4A). A high μ_{FE} above $45 \text{ cm}^2\text{V}^{-1}\text{s}^{-1}$ was achieved at V_{on} near -20 V , whereas cutting-edge techniques of the heterojunction oxide TFTs showed their average μ_{FE} at V_{on} of -40 V .^{23,24} The homojunction oxide TFTs consisting of amorphous CEML showed the similar tendencies of polycrystalline CEML, decreasing their average μ_{FE} of $25 \text{ cm}^2\text{V}^{-1}\text{s}^{-1}$ (Figure 3B and 4B).

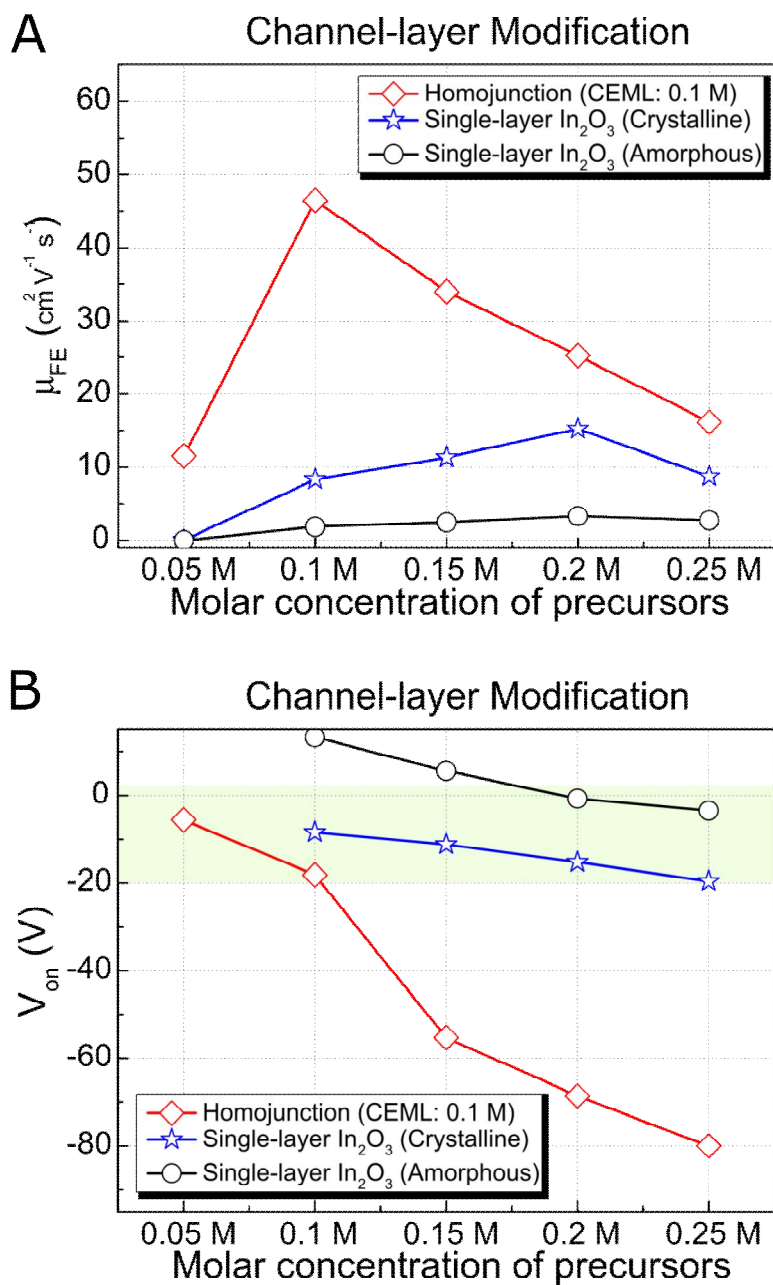
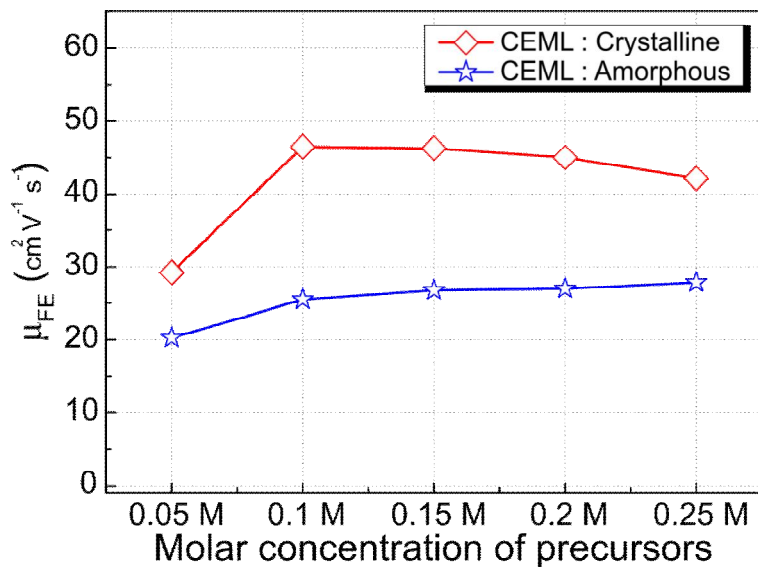


Figure 3. The inclination of Homojunction oxide TFTs for (A) μ_{FE} and (B) V_{on} depending on diverse conditions of channel layers.

A CEML Modification (Channel : 0.1 M crystalline)



B CEML Modification (Channel : 0.1 M crystalline)

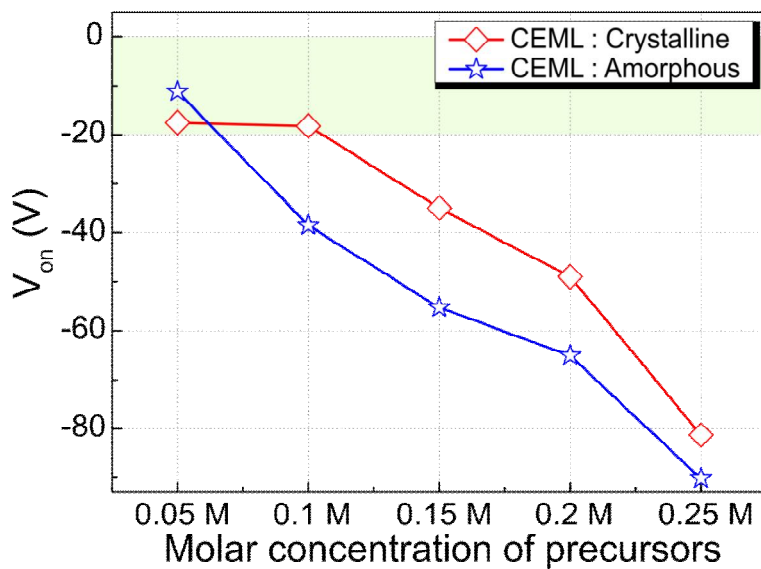


Figure 4. The tendency of Homojunction oxide TFTs toward (A) μ_{FE} and (B) V_{on} according to the modification of a CEML.

3.2.3 Admirable other traits: Stability and Uniformity

Not only did I accomplish highest μ_{FE} through the structure of homojunction, but I also demonstrated the stability of its electrical characteristics in long-term storage. Under ambient conditions, the solution-grown homojunction oxide TFTs kept their superior electrical performance more than 50 days, with both the V_{on} and μ_{FE} barely varied (Figure 5A). Another advantage of using the architecture of homojunction was the small μ_{FE} difference between solution-grown oxide TFTs. The uniformity of the homojunction oxide TFTs was illustrated by Figure 5B where the μ_{FE} of the 25 different homojunction devices was plotted as a function of product number. All solution-grown homojunction oxide TFTs represented little deviation between oxide TFTs' mobility with an average μ_{FE} of $46.5 \text{ cm}^2\text{V}^{-1}\text{s}^{-1}$, which is a remarkable advanced performance as compared to previous studies.

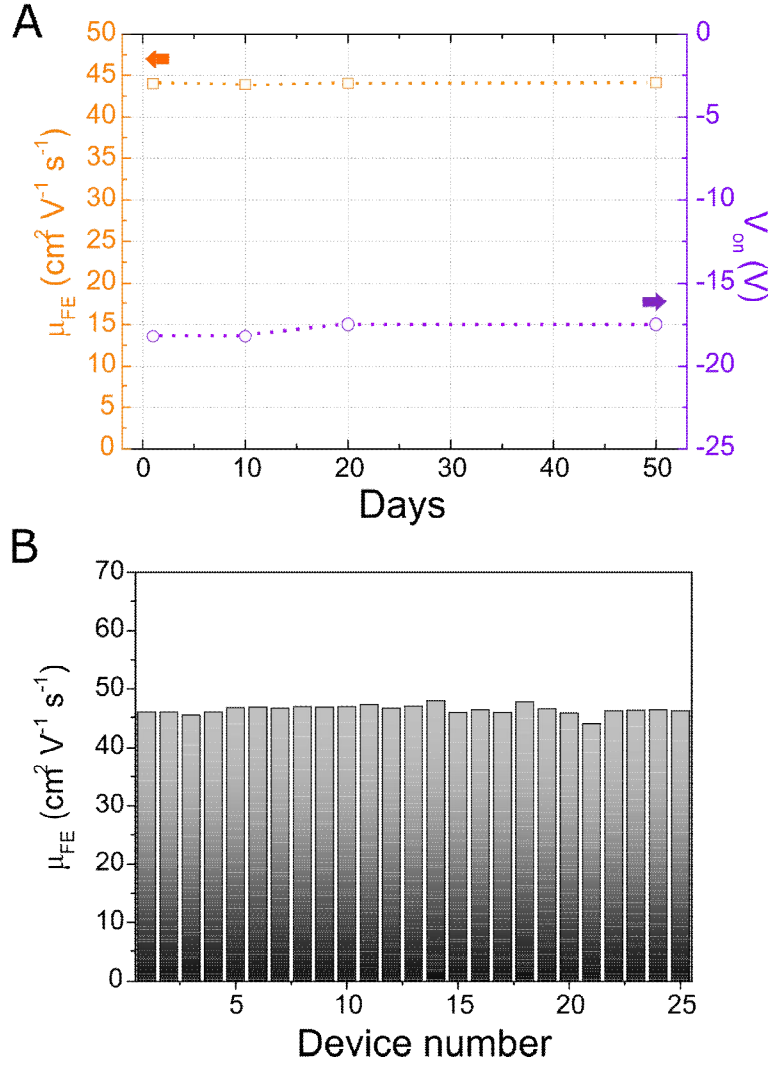


Figure 5. Reliability and uniformity of homojunction TFTs. (A) Electrical characteristics of homojunction lasting more than 50 days. (B) Histogram plot of μ_{FE} by 25 transistors of homojunction with In_2O_3 (0.1 M) / In_2O_3 (0.1 M).

3.3. Origin of the Outstanding Results

To elucidate the cause of these extraordinary outcomes from the solution-grown homojunction oxide TFTs, I performed a wide range of analyses such as x-ray diffraction (XRD), high-resolution transmission electron microscopy (HR-TEM), atomic force microscopy (AFM), x-ray photoelectron spectroscopy (XPS) and x-ray reflectivity (XRR).

3.3.1 Investigation in Phase of Thin Films by XRD

I implemented XRD analysis to find out if the phase of materials has an impact on the properties of the homojunction oxide TFTs. When the annealing temperature was at 250°C, Polycrystalline oxide thin films were formed. While other oxide thin films, annealed at 200°C, displayed amorphous phase (Figure 6). Although metal oxide films were produced in different phases depending on the annealing temperature, no huge differences were shown in the phases of the thin films which made from different molar concentrations precursors. The phases appeared to influence the solution-grown $\text{In}_2\text{O}_3/\text{In}_2\text{O}_3$ homojunction oxide TFTs in that their electrical performance with polycrystalline CEML was different from the ones with amorphous CEML, which have been discussed above.

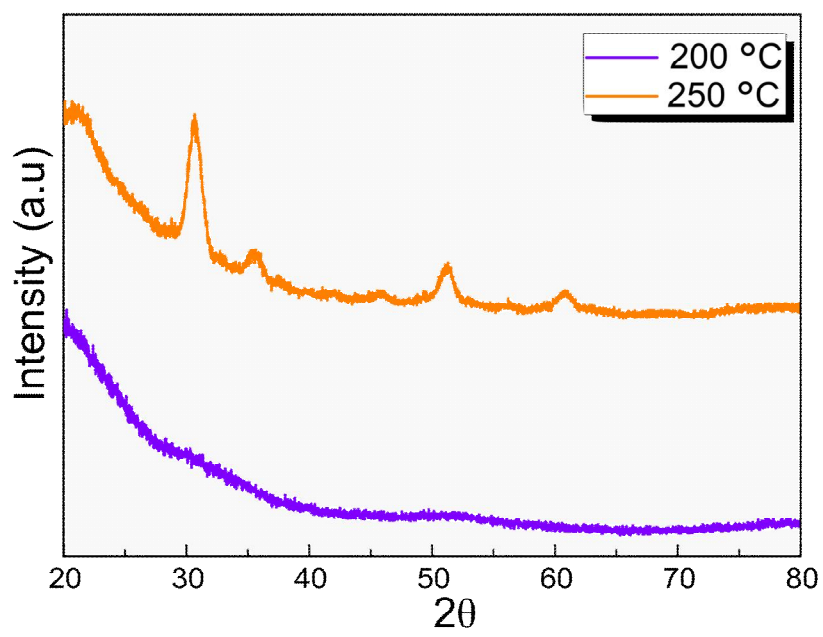


Figure 6. XRD characteristics of In_2O_3 films annealed at 250 °C and 200 °C.

3.3.2 Analysis of Homojunction through HR-TEM

HR-TEM analysis was carried out to further scrutinize the microstructure of the homojunction oxide thin films. The HR-TEM data afforded straightforward evidence that In_2O_3 thin films had phase of nanocrystalline with the lattice spacing of 0.41 nm. Also, the picture of HR-TEM showed the interfaces among CEML, channel-layer and dielectric layer were atomically sharp (Figure 7). Because the HR-TEM data demonstrated a low interface roughness of channel and supported a clue of the each layers not influencing each other, the electrical performance of the solution-grown homojunction oxide TFTs was considered to be affected by the channel layer.

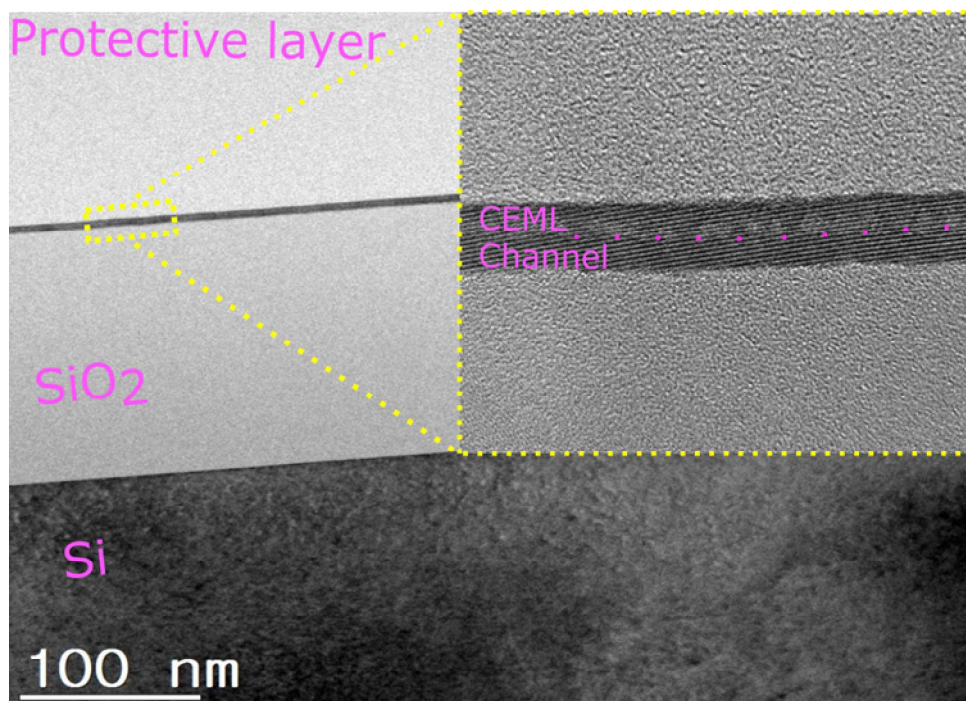


Figure 7. HR-TEM cross-section images of Si/SiO₂/In₂O₃ (0.1 M) / In₂O₃ (0.1 M) Homo Junction Oxide TFT.

3.3.3 Inquiry about Single Oxide Thin Film Layer via AFM and XPS

I scrutinized single-layered In_2O_3 thin films through AFM to examine the effect of a single layer itself. I figured out that molar concentrations of precursors had a linear relationship with film thicknesses, and its root mean square roughness (RRMS) showed atomically smooth topography for all In_2O_3 thin films (Figure 8 and Figure 9). These results were in accordance with the HR-TEM data representing a sharp interface between the CEML and the channel layer. Although the characteristics of oxide thin films such as the phase, RRMS and thicknesses depending on the molar concentration of precursors were identified, neither were the outstanding electrical performance sufficiently illustrated nor noticeable chemical and physical variances in oxide thin films were detected. Thus, I performed XPS analyses to unveil potential distinctions between oxide thin films depending on their precursors. The Outcomes of XPS did not represent remarkable changes in surface binding energy among the films. Nonetheless, notable differences were found when I examined the depth-resolved elemental composition of thick In_2O_3 thin film through successive XPS spectra at differing etching time (Figure 10). At the bulk region, the small amount of Si was detected due to the escape depth of the Si-2p photoelectrons, causing to the presence of Si at an etching time of ~ 100 s. The XPS data indicated that the amount of nitrogen gradually rose as etching time went by. Presumably, indium nitrate I used for making precursors caused this result. It is anticipated that nitrate components in the bulk region would not escape because of the dense film of surface formed by oxidation

(Figure 11A). This phenomenon was corroborated by former researches that notified a faster curing of the surface regions induce intermittent enclosure of precursors and solvent residues in the bulk areas of the layer and that revealed existence of surface skin layer on the poly methylsilsesquioxane surface (PMSSQ).^{28,36} In spite of presenting evidence of impurities being trapped, the source of a disparity in curing speed have been unknown. Also, previous studies have mainly implemented indirect methods to support this difference. My work proposed that rapid and dense surface regions were created mainly because of the oxidation phenomenon verified through O 1s XPS spectra (Figure 11B and 11C). Moreover, nitrogen elements are not removed during annealing process due to rapid reaction on the surface.

Furthermore, the escalated nitrogen element towards the bulk region appeared to degrade the electrical performance of the homojunction oxide TFTs since the nitrogen components performing as impurities hindered the coordination of indium and oxygen. In case of OSs, the bonding between metal and oxygen create percolated charge transport pathways.^{1,5,34} When atoms are distributed in their own periodic structure, considered as high density, the oxide TFTs show outstanding electrical characteristics. On the other hand, when impurities exist, they replace the positions for the constituents resulting in deformed structures, point defects or dislocations, all of which contribute to impeding the percolated transportation of carriers in OSs.^{15,19,28} Therefore, the higher the rate of impurities exists in the oxide thin film, the lower the oxide film densities achieve. The low density OS films induce inferior electrical performance of the oxide TFTs, which is in line with the electrical data of the homojunction oxide TFTs.

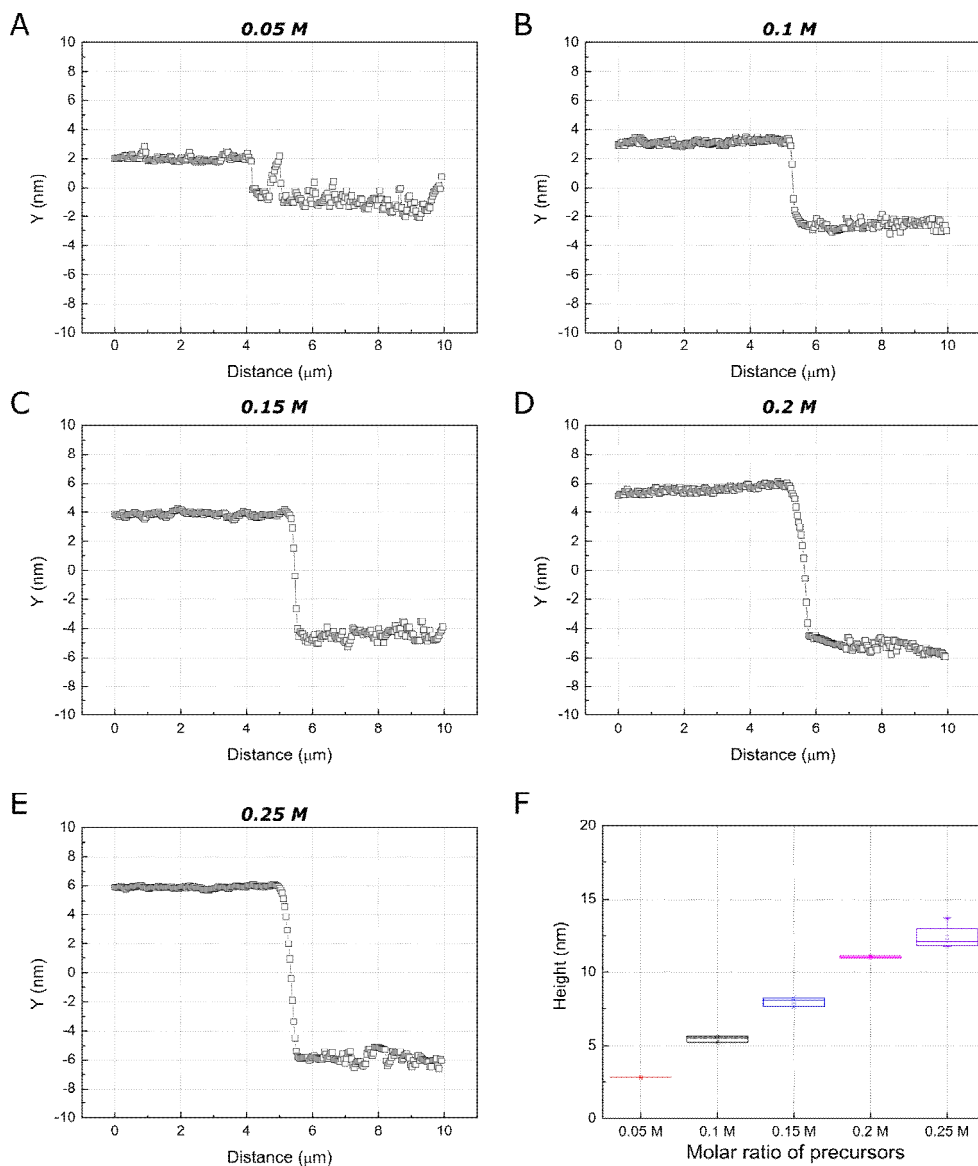


Figure 8. Height profile of various single-layered oxide thin films. (A) 0.05 M, (B) 0.1 M, (C) 0.15 M, (D) 0.2 M, (E) 0.25 M single-layered In_2O_3 thin films. (F) Height distributions derived from the AFM data.

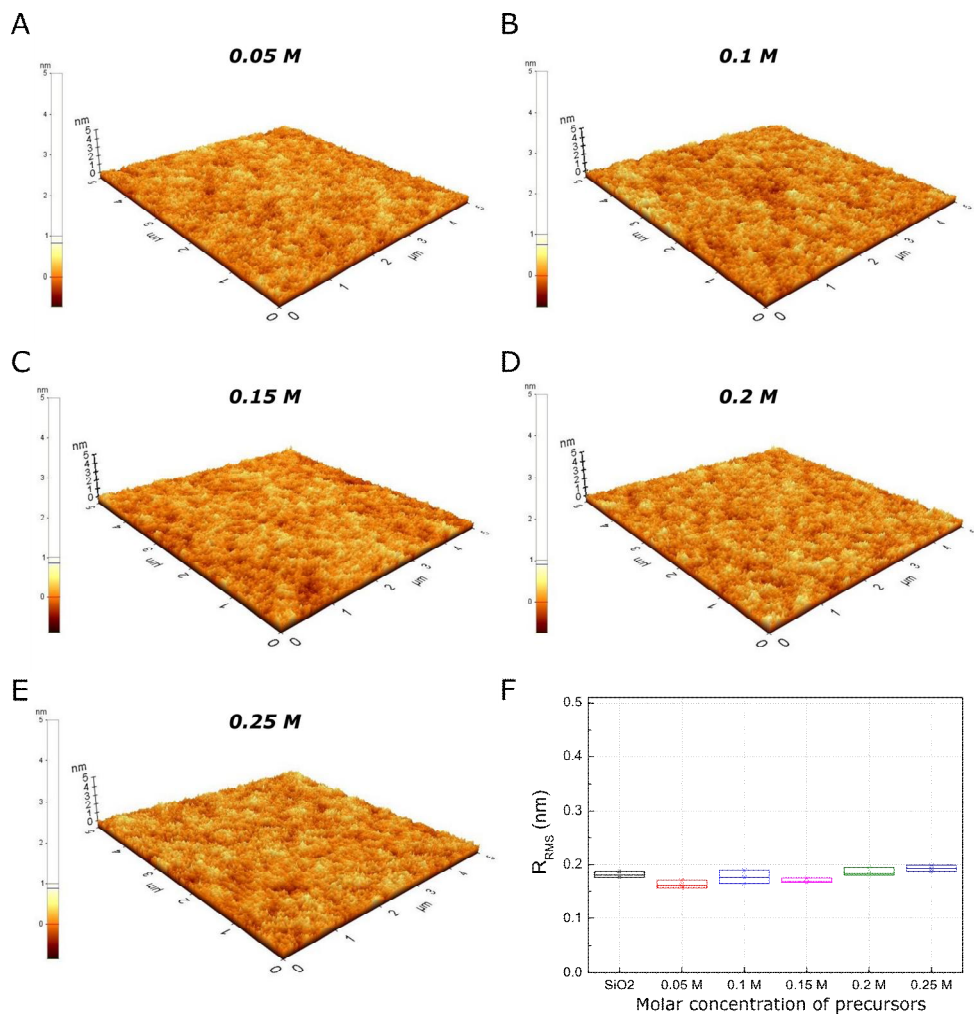


Figure 9. Surface topography of In_2O_3 thin films. (A) 0.05 M, (B) 0.1 M, (C) 0.15 M, (D) 0.2 M, (E) 0.25 M single-layered In_2O_3 thin films. (F) RMS distributions extracted from the AFM images.

Depth Profile of a 15 nm single-layered In_2O_3

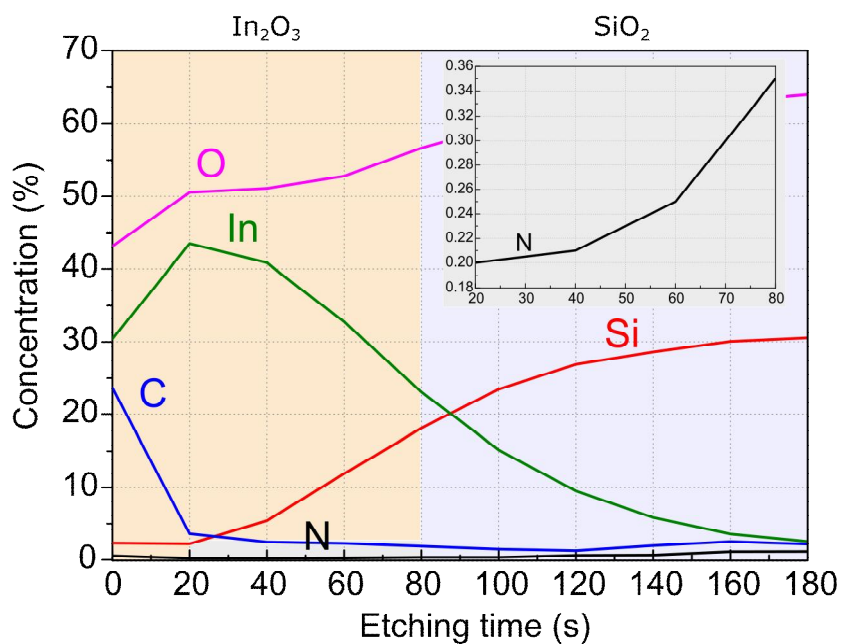


Figure 10. Elemental depth profile of the thick single-layered In_2O_3 thin film (~ 15 nm) stack on the Si/SiO_2 substrate.

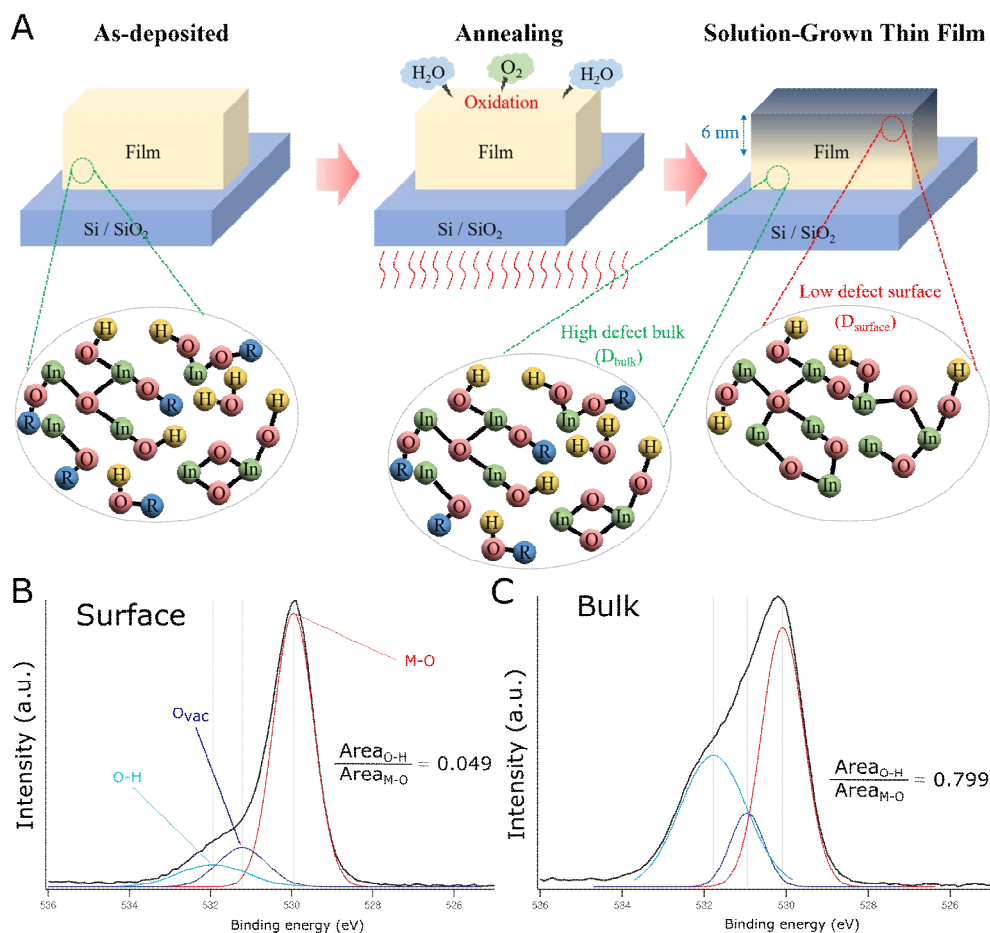


Figure 11. Process of a formation of solution-grown oxide thin films. (A) Schematic diagram from as-deposited to fully developed oxide films. XPS analysis of (B) surface and (C) bulk binding energy of 15 nm single-layered In_2O_3 thin films.

3.3.4 Examination of Density by using XRR

I further scrutinized single-layered In_2O_3 thin films by utilizing XRR to examine the density of various oxide thin films (Figure 12). As I predicted, the surface densities of all films were obtained with a value of 7.14 g/cm^3 similar to the density of an ideal indium oxide, which is 7.31 g/cm^3 .³³ On the contrary, the bulk region density decreased as the depth went deeper. Given the circumstances, I calculated the film density by adding the each density of surface and bulk, and then dividing it by the total thickness of respective film. The remarkable outcomes have been achieved in that solution-grown oxide thin films under 6 nm procured a density above 7.1 g/cm^3 , whereas ones above 6 nm displayed a lower density (Figure 12). This finding implies that the oxidation process at ambient conditions was interrupted when the oxide thin films were thicker than 6 nm, suggesting that solution-grown oxide films should be developed under 6 nm to produce high quality metal oxide layers.

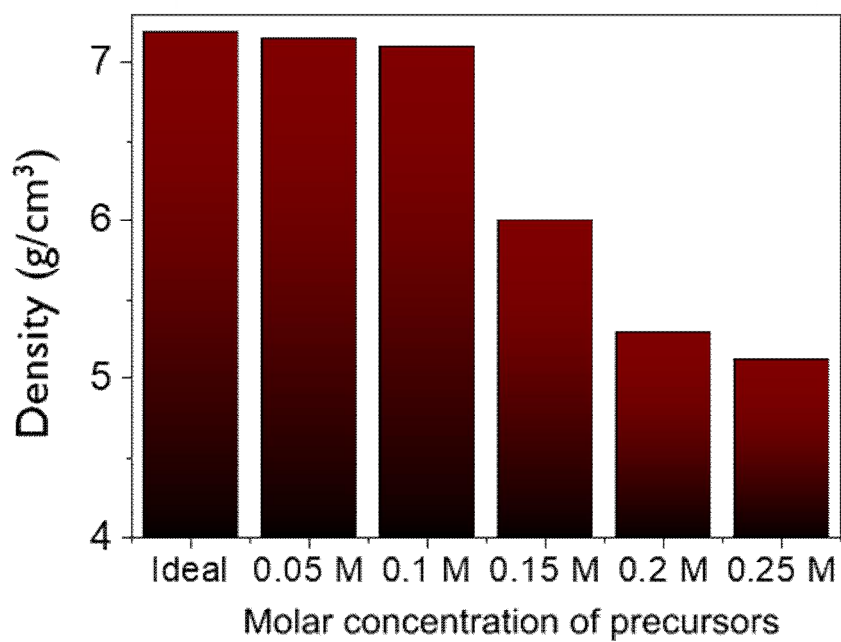


Figure 12. Density profile of single-layered In_2O_3 thin films depending on molar concentration of precursors.

3.4. Influences on Solution-Grown Oxide Thin Films

Based on the above analyzed data, the several impacts on solution-grown single-layered In_2O_3 and the $\text{In}_2\text{O}_3/\text{In}_2\text{O}_3$ homojunction oxide TFTs were summarized.

3.3.1 Single-Layered Oxide Thin Film

The single-layered In_2O_3 thin films under 11 nm represented inferior electrical performance because of a surface charge effect (Figure 13A). Charges trapped near the surface provoke the surface effect, affecting flowing charge carriers at the interface of the semiconductor-insulator by Coulomb forces.^{29,30} This leads to the attraction and repulsion of charges inside the channel. For this reason, the distance from surface to channel at least has to be larger than 7 nm to prevent trapping process or repulsion by surface charges.²⁹ In the case of single-layered In_2O_3 thin films above 11 nm, which is thick enough to avoid the surface charge effect, inferior electrical characteristics were stemmed from the impurities inside the bulk area (Figure 13B). Moreover, the hysteresis of single-layered In_2O_3 TFTs bolstered my assertion because V_{on} of the In_2O_3 TFTs with few defects (under 11 nm) barely changed while that of the highly defective In_2O_3 TFTs (above 11 nm) altered significantly.

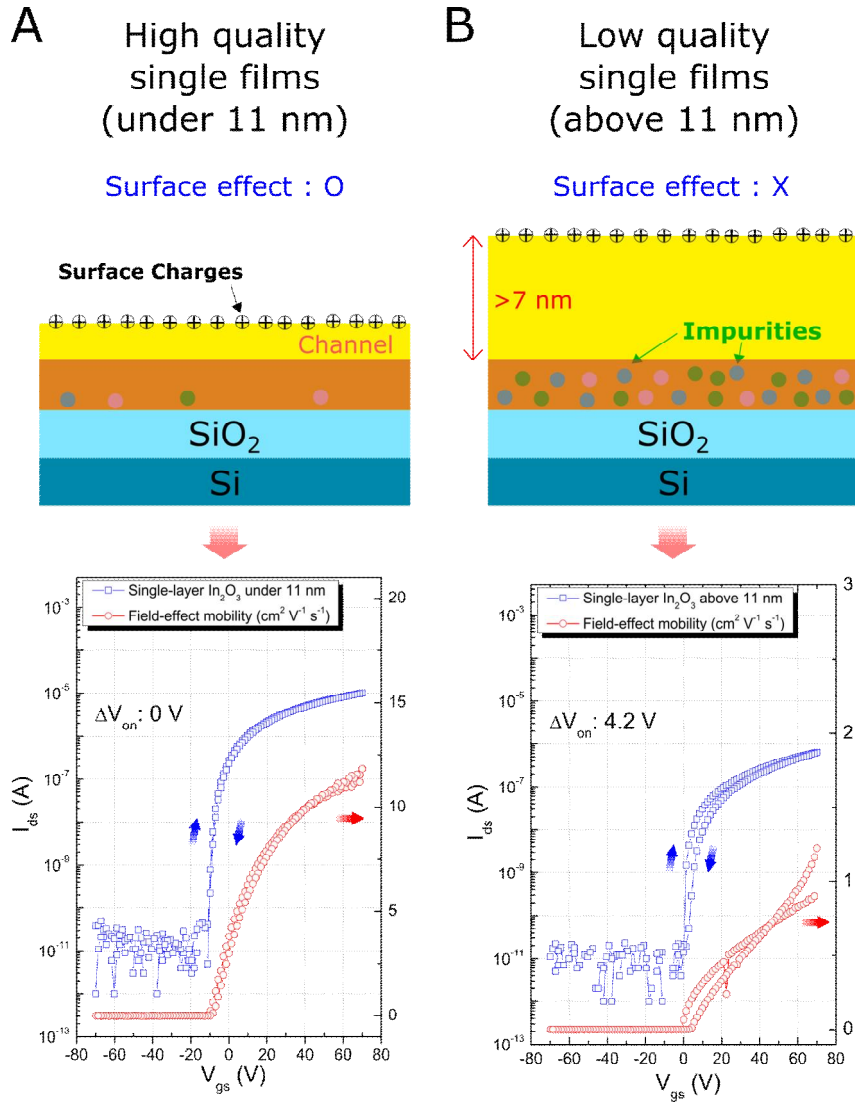


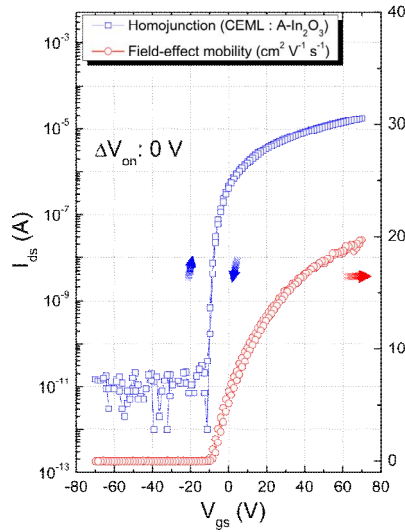
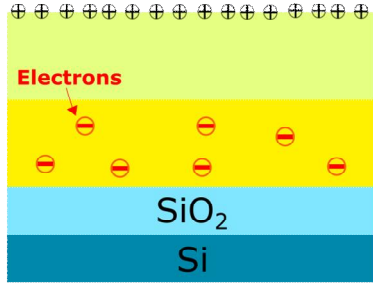
Figure 13. The influences of a surface charge effect and defects on single-layered oxide TFTs. Schematic images and electrical hysteresis of (A) High quality single films under 11 nm, (B) Low quality single films above 11 nm.

3.3.2 Homojunction Oxide Thin Film

The solution-grown homojunction oxide TFTs consisting of two high quality films, a CEML and a channel layer (~ 6 nm), were not affected by the surface effect and also displayed excellent hysteresis performance (Figure 14). The fermi level alignment occurs in case of amorphous CEML since amorphous In_2O_3 is likely to have a high work function compared to the polycrystalline In_2O_3 . When junction with two different phases happens, the charge carriers move from crystal to amorphous materials following the fermi level alignment. This causes to lower the carrier concentration in the channel. The mobility of the structure also decreased since the percolation and multiple trapping-and-release model are a conduction mechanism of OSs.^{1,5,34,35} On the other hand, the surface effect and the fermi level alignments were not discovered in the homojunction oxide TFTs with crystalline CEML, creating superior electrical performance.

A Homojunction
(CEML : A-In₂O₃)

Surface effect : X



B Homojunction
(CEML : C-In₂O₃)

Surface effect : X

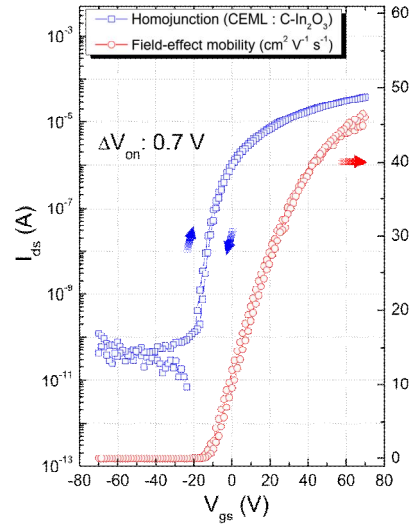
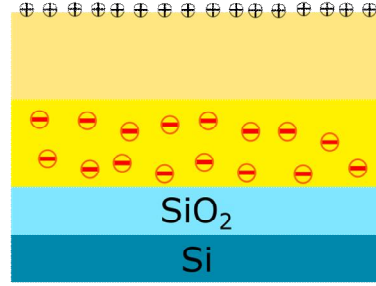


Figure 14. The impacts of defects and a surface charge effect on homojunction oxide TFTs. Schematic diagrams and electrical hysteresis of (A) homojunction TFTs with amorphous CEML (a-In₂O₃), and of (B) homojunction TFTs with crystalline CEML (C-In₂O₃)

3.5. Application: NMOS Inverter

I exploited these outstanding thin films to make an inverter which is one of the fundamental logic gates in logic circuits. An n-type metal oxide semiconductor (NMOS) inverter of depletion mode was fabricated by organizing the two homojunction TFTs made through solution process. A classical inverter performance was obtained where an output voltage in different voltage conditions varied from logic 0 to 1 depending on a swept input voltage (Figure 15). This suggested that the inverter consisting of solution-grown homojunction TFTs would also be suitable for integrating complex logic circuits.

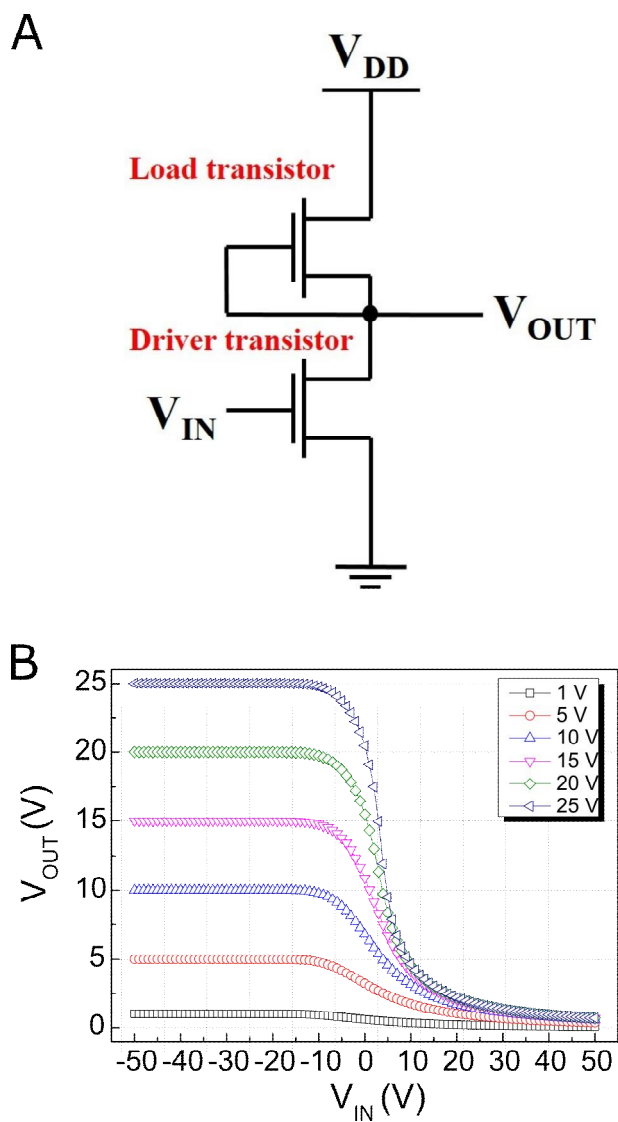


Figure 15. (A) Schematic architecture and (B) Voltage transfer characteristics of a solution-processed NMOS inverter consisting of two homojunction oxide TFTs.

Chapter 4. Conclusion

For the first time, low temperature solution-grown $\text{In}_2\text{O}_3/\text{In}_2\text{O}_3$ homojunction structure has been introduced by utilizing simple and low-cost deposition method. Despite exploiting the solution-grown oxide thin films, the homojunction oxide films displayed in this research achieved a remarkable electrical characteristics compared to other reported solution-grown oxide devices such as heterojunction oxide TFTs, zinc oxide TFTs and single-layered In_2O_3 . This research further grants several evidence on the electrical characteristics of solution-grown homojunction oxide TFTs, which is even similar to that of cutting-edge vacuum-processed devices.^{5,31,32} The phenomenal electrical performance of the solution-grown homojunction oxide TFTs is associated to three main points: (i) the roles of CEML to block the impact of surface space charges, (ii) the capability to control the charge carrier concentration in channel layer and therefore manipulate V_{on} , and (iii) the ability to make high quality oxide thin films through a solution process under ambient conditions. The most critical factor to achieve high μ_{FE} is producing high-quality oxide thin films, utilized for the channel layer. Because oxide thin films with low defects provide charge carrier paths, channel, of few impediments where charge carriers would easily flow. Moreover, the existence of CEML plays an important role in the solution-grown homojunction oxide TFTs since it helps to prevent the degradation of electrical characteristics stemmed from surface charge effect. Furthermore, manipulating the thickness and the phase of CEML

assist to achieve a semiconductor of tunable V_{on} and high mobility. Additionally, admirable other device traits such as uniformity and reliability are shown, for instance, the solution-grown homojunction oxide TFTs exhibit a long-term storage stability under ambient conditions. Overall, the homojunction architecture developed in this work have a huge potential for further usage in the advanced semiconductor industry. It also suggests that solution-grown OSs thin films will match favorably to mature semiconductor technologies in the near future if fabricated at a lower cost. This thesis was written based on the reported work, Junhee Lee *et al.* *ACS Applied Materials & Interfaces* **2019**, 11, 4103-4110.

References

1. K. Nomura, H. Ohta, A. Takagi, T. Kamiya, M. Hirano, H. Hosono, Room-temperature fabrication of transparent flexible thin-film transistors using amorphous oxide semiconductors. *Nature* **2004**, 432, 488–492.
2. E. M. C. Fortunato, P. M. C. Barquinha, A. C. M. B. G. Pimentel, A. M. F. Goncalves, A. J. S. Marques, R. F. P. Martins, L. M. N. Pereira, Wide-bandgap high-mobility ZnO thin-film transistors produced at room temperature. *Applied Physics Letters* **2004** 85, 2541–2543.
3. K. K. Banger, Y. Yamashita, K. Mori, R. L. Peterson, T. Leedham, J. Rickard, H. Sirringhaus, Low-temperature, high-performance solution-processed metal oxide thin-film transistors formed by a 'sol-gel on chip' process. *Nature Materials* **2011**, 10, 45–50.
4. E. Lee, J. Lee, J. H. Kim, K. H. Lim, J. S. Byun, J. Ko, Y. D. Kim, Y. Park, Y. S. Kim, Direct electron injection into an oxide insulator using a cathode buffer layer. *Nature Communication* **2015**, 6.
5. E. Fortunato, P. Barquinha, R. Martins, Oxide Semiconductor Thin-Film Transistors: A Review of Recent Advances. *Advanced Materials* **2012** 24, 2945–2986.
6. X. G. Yu, T. J. Marks, A. Facchetti, Metal oxides for optoelectronic applications. *Nature Materials* **2016**, 15, 383–396.
7. K. Kim, S. Park, J. B. Seon, K. H. Lim, K. Char, K. Shin, Y. S. Kim, Patterning of Flexible Transparent Thin-Film Transistors with Solution-Processed ZnO Using the Binary Solvent Mixture. *Advanced Functional Materials* **2011**, 21, 3546–3553.
8. E. Fortunato et al., Amorphous IZO TTFTs with saturation mobilities exceeding 100 cm²/Vs. *Physica Status Solidi–Rapid Research Letters* **2007**, 1, R34–R36.
9. S. J. Lim, S. J. Kwon, H. Kim, J. S. Park, High performance thin film transistor with low temperature atomic layer deposition nitrogen-doped ZnO. *Applied Physics Letters* **2007**, 91.

10. J. Jang, R. Kitsomboonloha, S. L. Swisher, E. S. Park, H. Kang, V. Subramanian, Transparent High-Performance Thin Film Transistors from Solution-Processed SnO₂/ZrO₂ Gel-like Precursors. *Advanced Materials* **2013**, 25, 1042–1047.
11. K. Nomura, H. Ohta, K. Ueda, T. Kamiya, M. Hirano, H. Hosono, Thin-film transistor fabricated in single-crystalline transparent oxide semiconductor. *Science* **2003**, 300, 1269–1272.
12. D. H. Lee, Y. J. Chang, G. S. Herman, C. H. Chang, A general route to printable high-mobility transparent amorphous oxide semiconductors. *Advanced Materials* **2007**, 19, 843–847.
13. W. Yang, K. Song, Y. Jung, S. Jeong, J. Moon, Solution-deposited Zr-doped AlO_x gate dielectrics enabling high-performance flexible transparent thin film transistors. *Journal of Materials Chemistry C* **2013**, 1, 4275–4282.
14. S. Park, C. H. Kim, W. J. Lee, S. Sung, M. H. Yoon, Sol-gel metal oxide dielectrics for all-solution-processed electronics. *Materials Science & Engineering R-Reports* **2017**, 114, 1–22.
15. K. H. Lim, J. Lee, J. E. Huh, J. Park, J. H. Lee, S. E. Lee, Y. S. Kim, A systematic study on effects of precursors and solvents for optimization of solution-processed oxide semiconductor thin-film transistors. *Journal of Materials Chemistry C* **2017**, 5, 7768–7776.
16. Y. H. Kim, J. S. Heo, T. H. Kim, S. Park, M. H. Yoon, J. Kim, M. S. Oh, G. R. Yi, Y. Y. Noh, S. K. Park, Flexible metal-oxide devices made by room-temperature photochemical activation of sol-gel films. *Nature* **2012**, 489, 128–132.
17. Y. G. Sun, J. A. Rogers, Inorganic semiconductors for flexible electronics. *Advanced Materials* **2007**, 19, 1897–1916.
18. M. G. Kim, M. G. Kanatzidis, A. Facchetti, T. J. Marks, Low-temperature fabrication of high-performance metal oxide thin-film electronics via combustion processing. *Nature Materials* **2011**, 10, 382–388.
19. Y. S. Rim, W. H. Jeong, D. L. Kim, H. S. Lim, K. M. Kim, H. J. Kim, Simultaneous modification of pyrolysis and densification for low-temperature solution-processed flexible oxide thin-film transistors. *Journal of Materials Chemistry* **2012**, 22,

12491–12497.

20. K. H. Lim, K. Kim, S. Kim, S. Y. Park, H. Kim, Y. S. Kim, UV–Visible Spectroscopic Analysis of Electrical Properties in Alkali Metal–Doped Amorphous Zinc Tin Oxide Thin–Film Transistors. *Advanced Materials* **2013**, 25, 2994–3000.
21. J. W. Jo, K. H. Kim, J. Kim, S. G. Ban, Y. H. Kim, S. K. Park, High–Mobility and Hysteresis–Free Flexible Oxide Thin–Film Transistors and Circuits by Using Bilayer Sol–Gel Gate Dielectrics. *Acs Applied Materials & Interfaces* **2018**, 10, 2679–2687.
22. Y. S. Rim, H. J. Chen, X. L. Kou, H. S. Duan, H. P. Zhou, M. Cai, H. J. Kim, Y. Yang, Boost Up Mobility of Solution–Processed Metal Oxide Thin–Film Transistors via Confining Structure on Electron Pathways. *Advanced Materials* **2014**, 26, 4273–4278.
23. D. Khim, Y. H. Lin, S. Nam, H. Faber, K. Tetzner, R. P. Li, Q. Zhang, J. Li, X. X. Zhang, T. D. Anthopoulos, Modulation–Doped In₂O₃/ZnO Heterojunction Transistors Processed from Solution. *Advanced Materials* **2017**, 29.
24. H. Faber, S. Das, Y. H. Lin, N. Pliatsikas, K. Zhao, T. Kehagias, G. Dimitrakopoulos, A. Amassian, P. A. Patsalas, T. D. Anthopoulos, Heterojunction oxide thin–film transistors with unprecedented electron mobility grown from solution. *Science Advances* **2017**, 3.
25. K. H. Lim, J. E. Huh, J. Lee, N. K. Cho, J. W. Park, B. I. Nam, E. Lee, Y. S. Kim, Strong Influence of Humidity on Low–Temperature Thin–Film Fabrication via Metal Aqua Complex for High Performance Oxide Semiconductor Thin–Film Transistors. *Acs Applied Materials & Interfaces* **2017**, 9, 548–557.
26. J. S. Park, J. K. Jeong, Y. G. Mo, H. D. Kim, C. J. Kim, Control of threshold voltage in ZnO–based oxide thin film transistors. *Applied Physics Letters* **2008**, 93.
27. P. Barquinha, A. Pimentel, A. Marques, L. Pereira, R. Martins, E. Fortunato, Influence of the semiconductor thickness on the electrical properties of transparent TFTs based on indium zinc oxide. *Journal of Non–Crystalline Solids* **2006**, 352, 1749–1752.

28. D. E. Walker, M. Major, M. Baghaie Yazdi, A. Klyszcz, M. Haeming, K. Bonrad, C. Melzer, W. Donner, H. von Seggern, High Mobility Indium Zinc Oxide Thin Film Field-Effect Transistors by Semiconductor Layer Engineering. *Acs Applied Materials & Interfaces* **2012**, 4, 6834–6840.
29. M. Ortel, S. Pittner, V. Wagner, Stability and spacial trap state distribution of solution processed ZnO–thin film transistors. *Journal of Applied Physics* **2013**, 113.
30. Y. Wang, X. W. Sun, G. K. L. Goh, H. V. Demir, H. Y. Yu, Influence of Channel Layer Thickness on the Electrical Performances of Inkjet-Printed In–Ga–Zn Oxide Thin-Film Transistors. *IEEE Transactions on Electron Devices* **2011**, 58, 480–485.
31. J. S. Park, W. J. Maeng, H. S. Kim, J. S. Park, Review of recent developments in amorphous oxide semiconductor thin-film transistor devices. *Thin Solid Films* **2012**, 520, 1679–1693.
32. L. Petti, N. Munzenrieder, C. Vogt, H. Faber, L. Buthe, G. Cantarella, F. Bottacchi, T. D. Anthopoulos, G. Troster, Metal oxide semiconductor thin-film transistors for flexible electronics. *Applied Physics Reviews* **2016**, 3.
33. C. T. Prewitt, R. D. Shannon, D. B. Rogers, A. W. Sleight, C rare earth oxide–corundum transition and crystal chemistry of oxides having the corundum structure. *Inorganic Chemistry* **1969**, 8, 1985–1993.
34. T. Kamiya, K. Nomura, H. Hosono, Origins of High Mobility and Low Operation Voltage of Amorphous Oxide TFTs: Electronic Structure, Electron Transport, Defects and Doping. *Journal of Display Technology* **2009**, 5, 273–288.
35. E. Lee, J. Ko, K. H. Lim, K. Kim, S. Y. Park, J. M. Myoung, Y. S. Kim, Gate Capacitance-Dependent Field-Effect Mobility in Solution-Processed Oxide Semiconductor Thin-Film Transistors. *Advanced Functional Materials* **2014**, 24, 4689–4697.
36. J. Bolze, M. Ree, H. S. Youn, S. H. Chu, K. Char, Synchrotron X-ray reflectivity study on the structure of templated polyorganosilicate thin films and their derived nanoporous analogues. *Langmuir* **2001**, 17, 6683–6691.

국문초록

우수한 전기특성을 지닌 용액공정 기반의 박막 트랜지스터

이 준 희

융합과학부 나노융합전공

서울대학교 대학원

최근 저온, 용액공정을 통하여 금속 산화물 박막 트랜지스터에 관심이 높아지고 있는데, 이는 저온, 용액공정이 유연하고 대면적 공정이 가능한 전자제품을 만드는데 적용할 수 있기 때문입니다. 그러나, 용액공정으로 만들어진 전자소자의 경우 낮은 전기적 특성을 갖거나 이러한 특성을 컨트롤하는데 많은 제약이 존재합니다. 이를 해결하기 위해, 우리는 “호모 접합”이라는 새로운 구조의 박막트랜지스터를 제안합니다. 이 호모접합 박막 트랜지스터는 현재까지 구현된 용액공정으로 만들어진 전자 소자보다 전기적 특성이 우수할 뿐만 아니라 이러한 특성들을 쉽게 조절이 가능합니다. 또한 용액공정으로 통해서 만들었음에도 불구하고, 안정성, 신뢰성 및 높은 일률을 갖고 있습니다. 우리의 연구결과는 낮은 어닐링 온도에서도 고품질의 박막을 얻을 수 있다는 것을 보여 주었고, 따라서 용액으로 성장한 트랜지스터 또한 광범위한 산업 응용 분야에 이용될 수 있음을 제시하고 있습니다.

주요어: 호모접합, 산화물 박막 트랜지스터, 용액공정, 고이동도, 턴온전압
학 번: 2017-26594